picCASO: A Cellular Automaton for Spatial Organisation

Sankalpa Venkatraghavan[1,2,†], Sathvik Anantakrishnan[1,2,†] and Karthik Raman[1,2,3,*]

[1]*Bhupat and Jyoti Mehta School of Biosciences, Department of Biotechnology, Indian Institute of Technology Madras, Chennai - 600 036, India*
[2]*Initiative for Biological Systems Engineering (IBSE), Indian Institute of Technology Madras, Chennai - 600 036, India*
[3]*Robert Bosch Centre for Data Science and Artificial Intelligence (RBCDSAI), Indian Institute of Technology Madras, Chennai - 600 036, India*

[†]These authors contributed equally
*Corresponding author. E-mail: kraman@iitm.ac.in

Abstract

Microbial consortia exhibit spatial patterning in several environments. However, the study of such patterning is limited by the inherent complexity of natural systems. An attractive alternative to study such systems involves the use of model synthetic microbial communities, which are convenient frameworks that allow the reuse of circuit components by eliminating cross-talk through compartmentalization of modules in genetic circuits. Computational models facilitate the understanding of how spatial organization can be harnessed as a tunable parameter in 2D cultures. We propose a Quorum Sensing-Mediated Model to engineer communication between strains in a consortium. This is implemented using a cellular automaton. We further analyze the properties of this model and compare them with those of the traditionally used Metabolite Mediated Model. Our studies indicate that modulating the rate of secretion of quorum sensing molecules is the most effective means of regulating community behavior. The models and codes are available from https://github.com/RamanLab/picCASO.

1 Introduction

Natural microbial communities exhibit spatial organisation in various niches. Examples include methanogens in mesophilic and thermophilic sludge granules (Sekiguchi et al., 1999), archaea in methane seep sediment (Dekas et al., 2014), nitrifying bacteria in soil aggregates (Nishio and Furusaka, 1970), the kelp bacterial community (Ramirez-Puebla et al., 2020) and the plant rhizosphere (Steidle et al., 2001). Spatial patterning is also observed in the human gut (Tropini et al., 2017), oral (Shrivastava et al., 2018) and skin (Bouslimani et al., 2015) microbiomes, where it is also hypothesized to have functional implications. The study of organisation in these natural communities is limited by the inherent complexity of the system and the variable physicochemical conditions. This has driven the design of synthetic communities (Tecon and Or, 2017; Zomorrodi and Segrè, 2016) and other *ex vivo* methods (Shrivastava et al., 2018) to mimic such natural conditions.

Advances in the field of synthetic biology have led to the development and deployment of functional systems composed of connected modular elements (Purnick and Weiss, 2009). A key feature of such systems is the interaction between such modules, which can be intracellular as in the case of gene circuits that cause cancerous cells to undergo apoptosis (Xie et al., 2011), or intercellular as in engineered mutualistic yeast strains (Shou et al., 2007). A significant challenge in building complex genetic circuits is the difficulty in reusing different circuit components within a cell, due to cross-talk. The distribution of genetic circuits *across* cells has been used to overcome this, and such compartmentalization requires engineering channels of communication (Regot et al., 2011). Spatial organization of cells can be used as a tunable parameter in these forms of distributed computing (Menon and Krishnan, 2019). Different strains have been designed to communicate with one another through the exchange of essential metabolites (Shou et al., 2007), or via quorum sensing (Kylilis et al., 2018).

Numerous mathematical models have been developed to study growth in two-dimensional microbial communities, as reviewed in Stubbendieck et al., 2016. Cellular automata have been used to model single species (Picioreanu et al., 1998) and multispecies (Chang et al., 2003) biofilm growth, fungal branching (Laszlo and Silman, 1993), bacterial colony morphologies (Ben-Jacob et al., 1994), yeast colony morphologies (Varahan et al., 2019) and colonization of surfaces by bacteria (Lloyd and Allen, 2015).

In this study, we explore two different models that are based on fitness modulation through intercellular communication. First, we propose a Quorum Sensing-Mediated Model (QSMM), which involves a novel synthetic microbial community comprising coupled single-gene deletion strains, whose growth rate is rescued upon quorum sensing by the expression of a deleted gene. For each strain in this community, sensing acyl-homoserine lactones (AHLs) secreted by a coupled strain leads to the expression of the deleted gene, thus restoring the growth rate of the deletion strain to that of the wild-type. This results in a system of coupled strains whose fitnesses are modulated through quorum sensing (Fig 1A). We developed a framework for the design of QSMM systems that involves the use of flux-balance analysis (FBA) to select genes for deletion. An orthogonal coupling paradigm is employed such that each strain senses QS molecules from one strain and secretes QS molecules that are sensed by another strain (Fig 1B). In contrast, the well-established Metabolite-Mediated Model (MMM; Shou et al., 2007) consists of a community of microbial strains, each of which is an auxotroph for an essential metabolite. Each coupled strain is capable of producing and secreting metabolites, which can be taken up by the other auxotroph. Thus, these auxotrophic strains cannot grow in the absence of their mutualistic counterparts.

Our models, available in the form of a MATLAB package, capture the dynamics of spatial organization in microbial consortia. They are implemented in the form of cellular automata and provide a framework to understand self-organization of cells in these communities. We use these models to study the most experimentally tractable parameters that can be used to tune system behavior. We also investigate the QSMM and MMM strategies employed to engineer intercellular communication and evaluate these in the context of our framework.

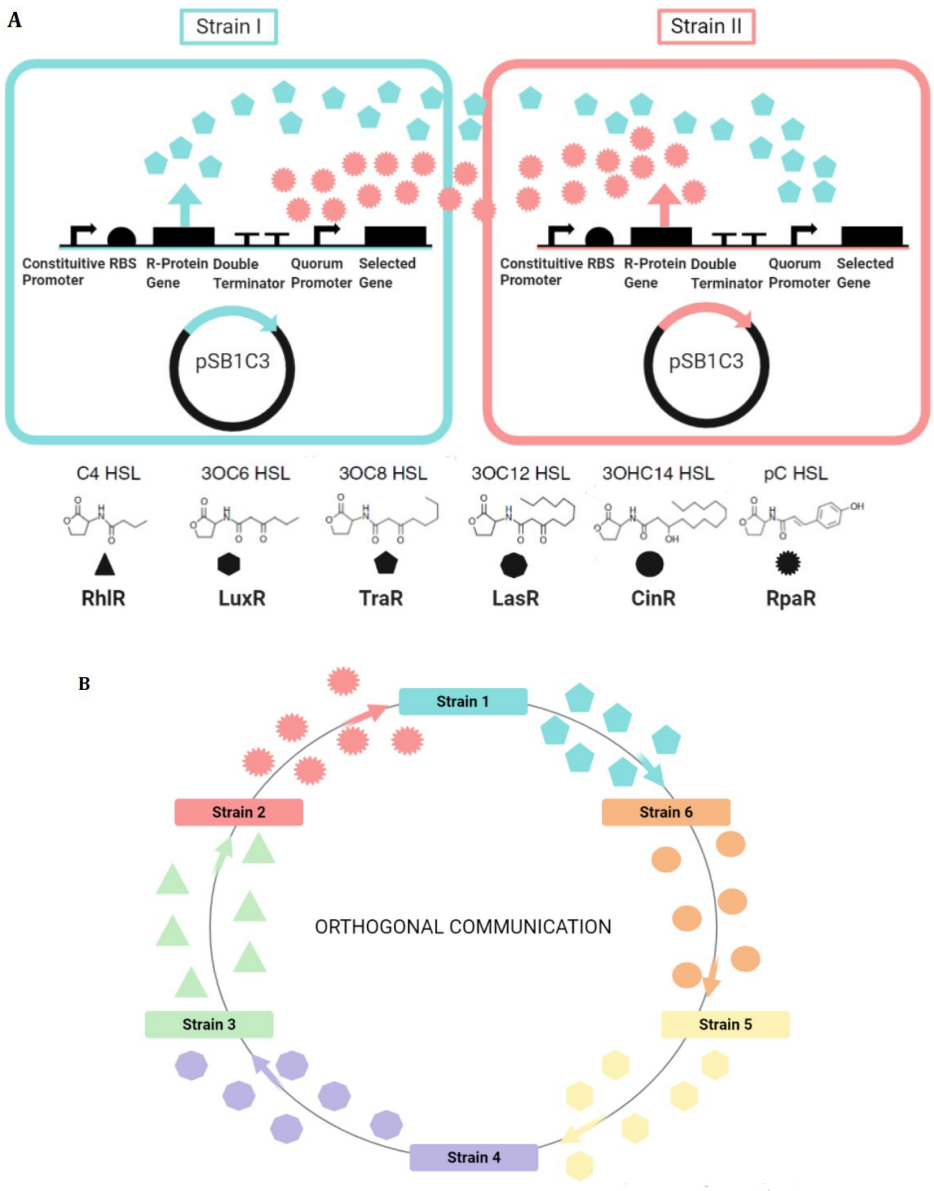

Figure 1: A schematic representation of the genetic circuit designed to implement the quorum sensing-mediated model (QSMM) for coupling bacterial strains using non-cognate acetyl-homoserine lactones and device pairs. (A) Strain I secretes 3OC8 HSL that affects gene expression in Strain II, through the activation of TraR. Strain II secretes pC HSL which affects gene expression in Strain I through the activation of RpaR. (B) A representation of possible orthogonal coupling between six strains, indicating how this paradigm can be extended to study any microbial community of interest. Quorum sensing molecules C4 HSL, 3OC6 HSL, 3OC8 HSL, 3OC12 HSL, 3OHC14 HSL and pC HSL are represented by triangles, hexagons, pentagons, octagons, circles and spiked circles respectively.

2 Methods

2.1 Model Framework

We implement the model on a two-dimensional grid, in which the nearest neighbours of each square in the grid are defined to be the four non-diagonally-adjacent squares. Cells of different types are seeded onto the grid in various configurations. The model has been implemented for two and three strains but is readily extendable to more strains. Each strain has an intrinsic base fitness associated with it. The associated fitnesses change as quorum sensing occurs because this leads to the expression of a gene that increases fitness. Cell division is assumed to occur probabilistically, based on the fitness of the cell. The diffusion of quorum sensing molecules is implemented using a Forward-Time Central-Space (FTCS) scheme (Roache, 1972).

$$U_{x,y,t+\Delta T} = U_{x,y,t} + D\,\Delta T/\Delta L2(\,U_{x-1,y,t} + U_{x+1,y,t} + U_{x,y-1,t} + U_{x,y+1,t} - 4U_{x,y,t})$$

where ΔT is the time step, ΔL is the space step or block length, and D is the diffusion constant for the resource.

2.2 Model Implementation

The model is implemented in MATLAB (Mathworks Inc., USA). Cell-blocks are defined using classes. The class contains methods to identify empty neighbouring blocks and simulate cell division. A strain's identity determines the amount and kind of quorum sensing molecules it releases. The model consists of grids that store the locations of the cells and the amounts of quorum sensing molecules in each block of the grid. In each iteration of the model, the cells seeded onto the grid release quorum sensing molecules. These molecules diffuse according to the FTCS scheme. The fitness of each cell is updated based on the concentration of quorum sensing molecules. Further, their degradation is assumed to follow first-order kinetics. Each cell block on the grid divides probabilistically. Cell blocks with higher fitnesses are thus more likely to divide in each step. This process can be iterated several hundreds of times depending on the time-scale of the processes to be simulated.

Flux Balance Analysis (FBA) is a technique used to predict the growth rate and metabolic capabilities of cells using genome-scale metabolic models (Raman and Chandra, 2009; Varma and Palsson, 1994). Under conditions of steady-state mass balance, FBA predicts the growth rate of cells and possible flux states that correspond to maximum growth. FBA can also be used to predict the phenotype of a cell following perturbations such as a gene deletion. We use FBA to predict the growth rate of cells, by optimizing for biomass. Using FBA, we characterize the growth of cells containing a single gene deletion, enabling us to define the cell's fitness. In our QSMM, communication between cells is engineered such that when a copy of the gene deleted in a strain is re-expressed through quorum sensing, the strain's fitness increases (back to its wild-type growth rate). Our simulations were performed using the COBRA Toolbox (Heirendt et al., 2019) for

MATLAB. We simulated single gene deletions *in silico* to predict the growth rate of strains in which a gene has been deleted, and compared it to the wild-type growth rate. A filtered growth ratio between a defined range (0.1–0.9) is used to select the genetic background of the strains used.

2.3 Model parameters

We introduce the concept of a cell block, as inspired by Varahan et al. (2019), who have previously used such cell blocks to model dynamics in yeast colonies. We assume that one cell block represents an area of 10 mm^2. This leads to a value of approximately 3×10^{-3} m for *dl*, the distance between adjacent cell blocks. Each block contains approximately 10^8 *E. coli* cells (Saint-Ruf et al., 2014). Further, it is assumed that all cells within a cell block have access to the entire resource pool within that cell block. Each time step in the model, *dt*, is 10 minutes. The rate of production of AHL molecules is 10^{-8} nmol per cell per hour (Marenda et al., 2016), which translates to a rate of secretion of 0.16 nmol per cell block per iteration. The diffusivity of AHLs in solid agar, *D*, is 8×10^{-10} m^2/s (Trovato et al., 2014). The diffusivity of metabolites is taken to be 5×10^{-10} m^2/s, which is the diffusivity of maltose (Nakanishi et al., 1977). The threshold amount of AHLs required to induce the expression of genes that cause a fitness change is approximately 1 nmol (Ramalho et al., 2016). The decay of AHL molecules follows first-order kinetics with a rate constant of approximately 0.00046 min^{-1} (Kaufmann et al., 2005). The fitness of a cell is defined as the time step per iteration (*dt* = 600 seconds) divided by the generation time. This leads to the cell dividing once per generation time on average. All parameter values used are listed in Supplementary Table 1.

For the QSMM, the base fitness used is determined based on the gene that is deleted. The wild-type fitness is calculated based on the generation time of the organism. The base fitness is taken to be the wild-type fitness multiplied by the growth ratio, which is the ratio of the biomass production rate of the knock-out strain to that of the wild-type. Quorum sensing leads to a gain in fitness such that the new fitness is equivalent to that of the wild-type strain. For the MMM, the base fitness is set at zero, as a strain cannot proliferate in the absence of an essential metabolite.

2.4 Choosing a genetic background

We identify potential candidate genes to be knocked out to obtain strains of interest through an FBA-based strategy employed on a genome-scale metabolic model. The genes whose deletion yields a growth ratio between 0.1 and 0.9 are selected. The *E. coli* iAF1260 model (Feist et al., 2007) is used by default. The gene list obtained for this model is given in Supplementary Table 2. This list enables the selection of the genetic background of strains used in further experiments. Once candidate genes are selected, the base fitness and gain in fitness are computed for each strain based on the generation time of the wild-type strain input by the user. Our models are available as a package on https://github.com/RamanLab/picCASO. It is possible to pick alternative models and other growth ratios for performing other simulations using our package.

Optimal communication can be engineered between different strains using a library of transcription factors and AHL pairs designed by Kylilis et al., 2018. The threshold concentrations to effect quorum sensing are obtained from this library. A list of predefined configurations including a random distribution of cells, cells arranged in parallel lines or a single file, cells seeded at diagonally opposite corners of a square, and cells arranged concentrically, are available for the user to select from. Alternatively, users may encode and analyze their patterns of interest.

3 Results

Our key results are four-fold. First, we validated our FTCS scheme for diffusion by reproducing a classic experiment that studied programmed pattern formation. Second, we established the validity of the model over an experimentally-tractable range of parameters. Third, we performed a parametric analysis to study the sensitivity of the system. Fourth, we compared the strengths of coupling between cells in two models of communications: the MMM and the QSMM.

3.1 The FTCS Scheme for Diffusion was Validated by Reproducing Experimental Results

To verify the diffusion scheme employed in our models, we replicated results from Basu et al. (2005). Weiss and co-workers developed a band-pass filter in which fluorescent proteins are only expressed within a narrow AHL concentration range. Their quantitative experiments were performed on a solid medium containing a lawn of bacteria sensing AHLs emitted by a "sender" colony seeded in the middle. In 36 hours, a steady-state was reached in which cells fluoresced in a ring between 5 mm and 18 mm from the sender colony (seen in Fig. 4a from Basu et al., 2005).

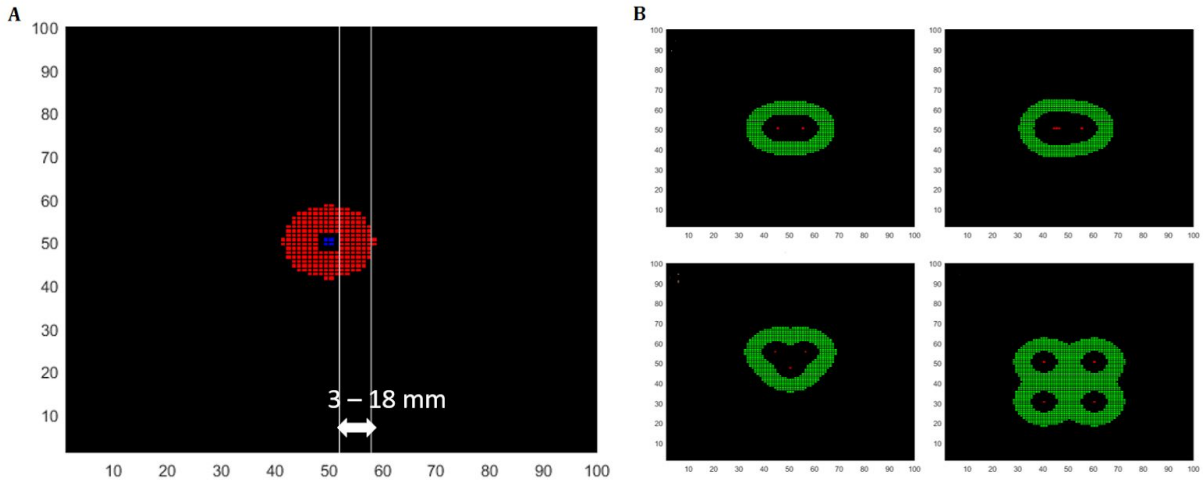

Figure 2: (A) Simulation results that capture the quantitative characteristics of the GFP bandpass filter in the AHL concentration range 0.01–0.2μM resulting in a band (shown in red) ranging from 3–18 mm from the sender colony (shown in blue). (B) Four patterns from Fig. 5 of Basu et al. (2005) have also been qualitatively reproduced.

We successfully reproduced this pattern using their parameter values and captured the same quantitative results. As seen in Fig. 2A, fluorescent gene expression was observed in the band spanning blocks 2 to 6 (3 mm to 18 mm) from the sender colony. The resolution of our coarse-grained model is 3 mm, which explains this discrepancy. Our model was also able to recreate several other patterns obtained in their qualitative experiments, including an ellipse, an oval, a heart, and a four-leafed clover (Fig. 2B; Fig. 5 from Basu et al., 2005).

3.2 Model Validity Was Observed Over The Experimentally Tractable Range of Parameters

We characterised our models using a "preferential growth assay", in which cells of two different strains were seeded in parallel lines, and the number of cell blocks dividing towards and away from the other strain was counted. When the model is functional, communication between the strains is expected to cause cell blocks of a strain to preferentially proliferate toward cell blocks of the other strain. The absence of preferential growth indicates the decoupling of the strains.

We chose to vary the parameters that are most amenable to experimental modification, namely, the rate of secretion of QS molecules (which can be modulated using promoters of differing strengths); the threshold concentration of QS molecules to cause QS-dependent gene expression (which can be varied using different AHL/device pairs); the gain in fitness upon quorum sensing (which can be varied by using different strains as suggested by our FBA-based design). Here, the term device refers to the combination of the gene encoding a transcription factor that senses a particular AHL and the promoter whose expression is driven by that transcription factor. These parameters were varied over ranges that have previously been observed in experiments (see Supplementary Table S2 for details). We observe that for all three parameters studied (Fig.3B, Fig. S1B, Fig. S2B), significant preferential growth is seen across the entire range being considered. This demonstrates our model validity and the absence of model breakdown over all experimentally tractable ranges of parameters.

3.3 Rate of Secretion of Quorum Sensing Molecules Best Modulates Model Behavior

To study the parameter space in the two-strain model, we performed a grid search and analyzed the effect of the variation of parameters of one strain on the resulting relative populations of cells, with the parameters corresponding to the other strain kept constant. Initially, four cell blocks of each strain were seeded randomly on the grid and allowed to proliferate for 50 iterations, corresponding to 500 minutes. This was repeated over 100 runs of the model.

From Fig. 3A, which visualises the variation in the number of cells of a strain with respect to the parameters of interest, we observed that when the rate of secretion of Strain 1 (the strain whose parameters are being varied) is very high, Strain 2 enjoys an advantage irrespective of the other parameter values. This trend of the advantage gained by the strain coupled to a strain with a higher rate of secretion is observed in the studied parameter ranges. This is to be expected, since the rate

of secretion of QS molecules from a strain results in a fitness gain for the coupled strain sooner and over a greater area around cells of the first strain.

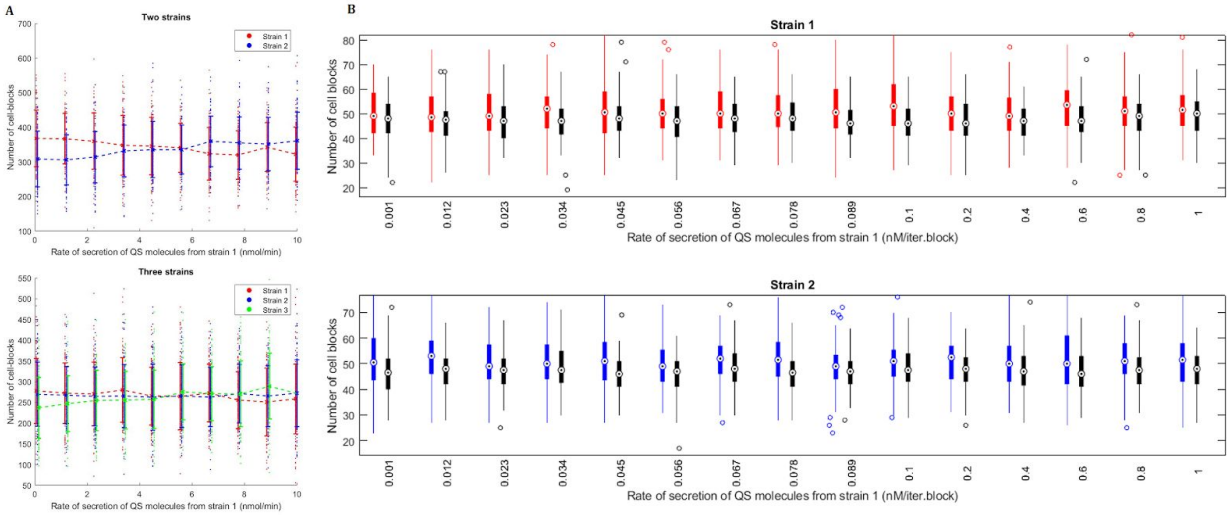

Figure 3: (A) The populations of each strain in the two (above) and three (below) strain QSMM models with the rate of secretion of AHL molecules from strain 1 being varied and the rate of secretion from the other strain(s) kept constant at 5 nmol/min. (B) Preferential growth assay quantifying the number of cell blocks of strain 1 (above) and strain 2 (below) dividing towards (shown in colour) and away from (shown in black) cell blocks of the other strain with the rate of secretion of AHL molecules from strain 1 being varied and the rate of secretion from the other strain(s) kept constant at 5 nmol/min

To obtain a more fine-grained picture of the above results, we varied each parameter individually over the same range with 4 cell blocks initially seeded randomly on the grid and allowed it to proliferate for 100 iterations (1000 minutes) for 100 runs of the model. These simulations were run for 2-strain and 3-strain models. Consistent with the above results, we see that a higher rate of secretion from one strain led to an increase in the number of cells of the type it was engineered to communicate with. Changing the threshold amount of AHLs required for gene expression yielded a high number of cells of a strain at very low thresholds for that strain. However, the number of cells of all strains rapidly converged to nearly equal values when the threshold was increased. This may be because the threshold values are too high to provide a fitness advantage resulting in a situation where cell division is dependent only on the base fitness –– which is equal for all strains. Variation of the gain in fitness upon quorum sensing shows no discernible pattern, perhaps due to the stochastic nature of the processes involved. Therefore, we observe that among the parameters considered, tuning the rate of secretion of quorum sensing molecules is most advantageous to regulate model behavior.

To examine the effects of stochasticity in the model, we visualised relative populations of cell blocks of the two strains from each of the 12,500 runs of the grid search, as shown in Fig. 4B. A wide spread was observed in the data, and this variation was present even at the scale of one parameter set.

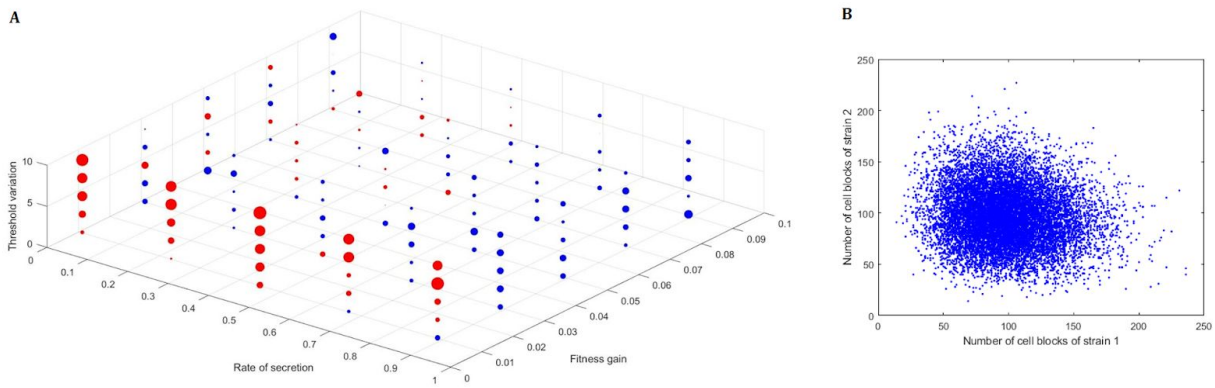

Figure 4: (A) A 3D plot that depicts the variation in the number of cell blocks of a strain with respect to the rate of secretion of QS molecules, the gain in fitness and variation in threshold concentration needed to induce gene expression in the QSMM model with two strains. The colour of every point in the plot is determined by the strain with the higher number of cell blocks while its size is proportional to the difference between the number of cell blocks of each strain. (B) A plot depicting the variation in relative populations of strains 1 and 2 across 12,500 runs of the model.

3.4 MMM Demonstrates Greater Coupling than QSMM

To investigate how the mode of communication between microbes in a consortium affects spatial organisation, we compared the strength of coupling between strains in the MMM and the QSMM. Our QSMM models were modified to arrive at the MMM such that the fitness of a strain in the absence of the coupled strain is nil. This is due to the inability of the strain to produce an essential metabolite. In the presence of communication with the coupled strain, the fitness returns to that of the wild type value due to uptake of the essential metabolite secreted by the coupled strain.

It was seen that cell–cell communication in both the QSMM and the MMM led to increases in cell fitness. This was quantified through the preferential growth assay. We observed that in both models, cells grew preferentially towards cells of the other type and this coupling was noted to be statistically significant, and stronger in the case of the MMM (Fig. 5).

4 Discussion

In the study of synthetic microbial consortia, the ability to engineer spatial organisation allows for the compartmentalization of different functional genetic circuits. This is an effective means of reducing both the biochemical crosstalk and the complexity of synthetic genetic circuits within a single strain. A direct consequence of this is the ability to build more sophisticated and targeted gene circuits. The study of synthetic consortia can provide valuable insights into the behaviour of natural microbial consortia by serving as a model system. It enables the investigation of natural microbial communities that are spatially organised and also provides a means to study the population dynamics of consortia. Our models facilitate the use of spatial organisation as a tunable

parameter in synthetic biology by engineering communication based on the location and strength of coupling of microbial strains.

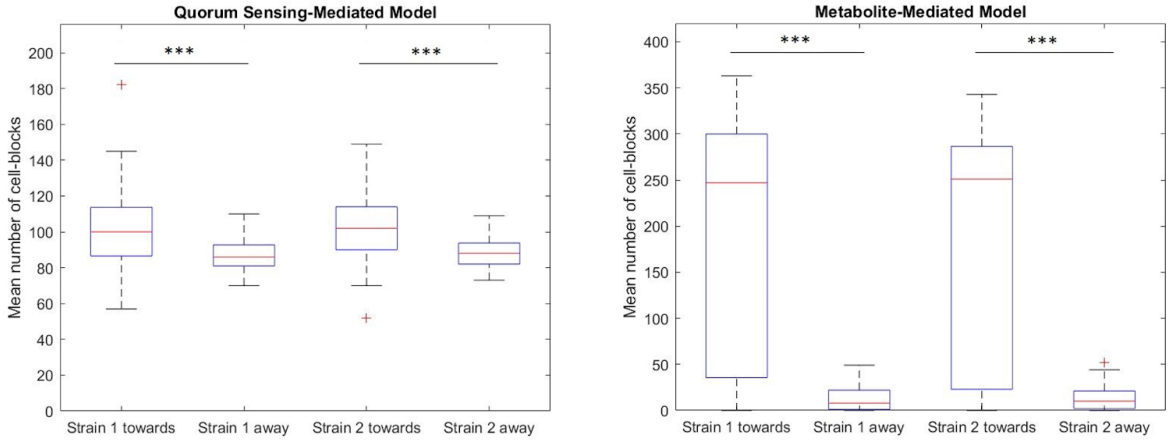

Figure 5: Comparison of the QSMM (left) and the MMM (right) through quantification of the number of cell blocks of a given strain that divide towards and away from the second strain in a 2 strain model using the preferential growth assay. For the QSMM, $p=10^{-11}$ for strain 1 and $p=10^{-12}$ for strain 2. For the MMM, $p=10^{-24}$ for strain 1 and $p=10^{-23}$ for strain 2.

Through our study of different models of communication, we concluded that strains are more strongly coupled in the MMM compared to the QSMM. This can be understood intuitively as the MMM uses auxotrophic strains whose base fitness, in the absence of the mutualistic strain, is zero. In the QSMM, on the other hand, strains have a low but non-zero base fitness even in the absence of other strains. However, an important point to note is that the design of systems using the QSMM is more experimentally tractable. It is much easier to couple several bacterial strains using non-cognate AHL/TF pairs than it is to build a network of mutually-dependent auxotrophs whose relative populations are well-regulated. The design of systems using the QSMM is further simplified by the availability of a well-characterized library of AHL/TF pairs curated by Kylilis et al., 2018, with a MATLAB package to select appropriate devices.

A limitation of our models is that they do not account for intercellular dynamics, and thus cannot accurately recapitulate some aspects of temporal dynamics. Currently, the model is coarse-grained and does not take into account the dynamics of gene regulation, which manifests as an absence of a time delay in the replicated results from Basu et al., (2005). Our models also consider gene expression due to quorum sensing to be a Boolean process gated by a threshold. As a result, different AHL concentrations greater than the threshold are not considered when QS mediated gene expression and fitness values are varied. However, it is possible to extend our model to account for gene regulatory dynamics.

Our models are available as an easy-to-use MATLAB package, which can be used in conjunction with the tool developed by Kylilis et al., 2018. The AHL/ device pairs selected can be inputted to our

package to analyse spatial organisation. We have demonstrated its extendibility to multiple strains whose communication is engineered in an orthogonal fashion and shown that the QSMM allows for coupling of strains throughout the entire range of experimentally tractable values. This provides a theoretical basis to understand the self-organization of cells in a microbial community. The model can be fine-tuned with the incorporation of intercellular dynamics and metabolic constraints. An extension of our work would be to develop tools to suggest initial seed configurations to arrive at patterns of interest. Such a tool would provide predictive power to our model and allow experimentalists to generate patterns of interest.

To summarise, our study provides a versatile model that can be used to study spatial patterning in microbial communities. We show that our QSMM approach can be a powerful tool to manipulate community behaviour. The models can be harnessed to predict the initial seed configuration to arrive at characterised patterns of interest. Our model can be easily extended to study the configurations of cells required to implement distributed cellular computing, and the organisation of microbiomes, biofilms, and other natural microbial communities.

Acknowledgements

KR acknowledges support from the Science and Engineering Board (SERB) MATRICS Grant MTR/2020/000490, IIT Madras, Initiative for Biological Systems Engineering (IBSE) and Robert Bosch Center for Data Science and Artificial Intelligence (RBC-DSAI). SA acknowledges The Department of Science and Technology (DST) for the INSPIRE Scholarship for Higher Education (SHE). The authors acknowledge the use of the computing resources at HPCE, IIT Madras. The authors are grateful to Dr. Gayathri Sambamoorthy for inputs regarding data visualisation and Vibha Balaji for copy editing the manuscript.

References

Basu, S., Gerchman, Y., Collins, C.H., Arnold, F.H., Weiss, R., 2005. A synthetic multicellular system for programmed pattern formation. Nature 434, 1130–1134. https://doi.org/10.1038/nature03461

Bouslimani, A., Porto, C., Rath, C.M., Wang, M., Guo, Y., Gonzalez, A., Berg-Lyon, D., Ackermann, G., Moeller Christensen, G.J., Nakatsuji, T., Zhang, L., Borkowski, A.W., Meehan, M.J., Dorrestein, K., Gallo, R.L., Bandeira, N., Knight, R., Alexandrov, T., Dorrestein, P.C., 2015. Molecular cartography of the human skin surface in 3D. Proc. Natl. Acad. Sci. U. S. A. 112, E2120–E2129. https://doi.org/10.1073/pnas.1424409112

Dekas, A.E., Chadwick, G.L., Bowles, M.W., Joye, S.B., Orphan, V.J., 2014. Spatial distribution of nitrogen fixation in methane seep sediment and the role of the ANME archaea. Environ. Microbiol. 16, 3012–3029. https://doi.org/10.1111/1462-2920.12247

Feist, A.M., Henry, C.S., Reed, J.L., Krummenacker, M., Joyce, A.R., Karp, P.D., Broadbelt, L.J., Hatzimanikatis, V., Palsson, B.Ø., 2007. A genome-scale metabolic reconstruction for Escherichia coli K-12 MG1655 that accounts for 1260 ORFs and thermodynamic information. Mol. Syst. Biol. 3, 121. https://doi.org/10.1038/msb4100155

Heirendt, L., Arreckx, S., Pfau, T., Mendoza, S.N., Richelle, A., Heinken, A., Haraldsdóttir, H.S.,

Wachowiak, J., Keating, S.M., Vlasov, V., Magnusdóttir, S., Ng, C.Y., Preciat, G., Žagare, A., Chan, S.H.J., Aurich, M.K., Clancy, C.M., Modamio, J., Sauls, J.T., Noronha, A., Bordbar, A., Cousins, B., El Assal, D.C., Valcarcel, L.V., Apaolaza, I., Ghaderi, S., Ahookhosh, M., Ben Guebila, M., Kostromins, A., Sompairac, N., Le, H.M., Ma, D., Sun, Y., Wang, L., Yurkovich, J.T., Oliveira, M.A.P., Vuong, P.T., El Assal, L.P., Kuperstein, I., Zinovyev, A., Hinton, H.S., Bryant, W.A., Aragón Artacho, F.J., Planes, F.J., Stalidzans, E., Maass, A., Vempala, S., Hucka, M., Saunders, M.A., Maranas, C.D., Lewis, N.E., Sauter, T., Palsson, B.Ø., Thiele, I., Fleming, R.M.T., 2019. Creation and analysis of biochemical constraint-based models using the COBRA Toolbox v.3.0. Nat. Protoc. 14, 639–702. https://doi.org/10.1038/s41596-018-0098-2

Kaufmann, G.F., Sartorio, R., Lee, S.H., Rogers, C.J., Meijler, M.M., Moss, J.A., Clapham, B., Brogan, A.P., Dickerson, T.J., Janda, K.D., 2005. Revisiting quorum sensing: Discovery of additional chemical and biological functions for 3-oxo-N-acylhomoserine lactones. Proc. Natl. Acad. Sci. U. S. A. 102, 309–314. https://doi.org/10.1073/pnas.0408639102

Kylilis, N., Tuza, Z.A., Stan, G.B., Polizzi, K.M., 2018. Tools for engineering coordinated system behaviour in synthetic microbial consortia. Nat. Commun. 9, 1–9. https://doi.org/10.1038/s41467-018-05046-2

Marenda, M., Zanardo, M., Trovato, A., Seno, F., Squartini, A., 2016. Modeling quorum sensing trade-offs between bacterial cell density and system extension from open boundaries. Sci. Rep. 6. https://doi.org/10.1038/srep39142

Menon, G., Krishnan, J., 2019. Design Principles for Compartmentalization and Spatial Organization of Synthetic Genetic Circuits. ACS Synth. Biol. 8, 1601–1619. https://doi.org/10.1021/acssynbio.8b00522

Nakanishi, K., Adachi, S., Yamamoto, S., Matsuno, R., Tanaka, A., Kamikubo, T., 1977. Diffusion of Saccharides and Amino Acids in Cross-linked Polymers. Agric. Biol. Chem. 41, 2455–2462. https://doi.org/10.1080/00021369.1977.10862880

Nishio, M., Furusaka, C., 1970. The distribution of nitrifying bacteria in soil aggregates. Soil Sci. Plant Nutr. 16, 24–29. https://doi.org/10.1080/00380768.1970.10432820

Purnick, P.E.M., Weiss, R., 2009. The second wave of synthetic biology: From modules to systems, Nature Reviews Molecular Cell Biology. Nature Publishing Group. https://doi.org/10.1038/nrm2698

Ramalho, T., Meyer, A., Mückl, A., Kapsner, K., Gerland, U., Simmel, F.C., 2016. Single cell analysis of a bacterial sender-receiver system. PLoS ONE 11. https://doi.org/10.1371/journal.pone.0145829

Raman, K., Chandra, N., 2009. Flux balance analysis of biological systems: applications and challenges. Brief. Bioinform. 10, 435–449. https://doi.org/10.1093/bib/bbp011

Ramirez-Puebla, S.T., Weigel, B.L., Jack, L., Schlundt, C., Pfister, C.A., Welch, J.L.M., 2020. Spatial organization of the kelp microbiome at micron scales. bioRxiv 2020.03.01.972083. https://doi.org/10.1101/2020.03.01.972083

Regot, S., Macia, J., Conde, N., Furukawa, K., Kjellén, J., Peeters, T., Hohmann, S., de Nadal, E., Posas, F., Solé, R., 2011. Distributed biological computation with multicellular engineered networks. Nature 469, 207–211. https://doi.org/10.1038/nature09679

Roache, P., 1972. Computational Fluid Dynamics. Hermosa Publishers, Albuquerque NM.

Saint-Ruf, C., Garfa-Traoré, M., Collin, V., Cordier, C., Franceschi, C., Matic, I., 2014. Massive diversification in aging colonies of Escherichia coli. J. Bacteriol. 196, 3059–3073. https://doi.org/10.1128/JB.01421-13

Sekiguchi, Y., Kamagata, Y., Nakamura, K., Ohashi, A., Harada, H., 1999. Fluorescence in situ hybridization using 16S rRNA-targeted oligonucleotides reveals localization of methanogens and selected uncultured bacteria in mesophilic and thermophilic sludge granules. Appl. Environ. Microbiol. 65, 1280–1288. https://doi.org/10.1128/AEM.65.3.1280-1288.1999

Shou, W., Ram, S., Vilar, J.M.G., 2007. Synthetic cooperation in engineered yeast populations. Proc. Natl. Acad. Sci. U. S. A. 104, 1877–1882. https://doi.org/10.1073/pnas.0610575104

Shrivastava, A., Patel, V.K., Tang, Y., Yost, S.C., Dewhirst, F.E., Berg, H.C., 2018. Cargo transport shapes the spatial organization of a microbial community. Proc. Natl. Acad. Sci. 115, 8633–8638. https://doi.org/10.1073/pnas.1808966115

Steidle, A., Sigl, K., Schuhegger, R., Ihring, A., Schmid, M., Gantner, S., Stoffels, M., Riedel, K., Givskov, M., Hartmann, A., Langebartels, C., Eberl, L., 2001. Visualization of N-Acylhomoserine Lactone-Mediated Cell-Cell Communication between Bacteria Colonizing the Tomato Rhizosphere. Appl. Environ. Microbiol. 67, 5761–5770. https://doi.org/10.1128/AEM.67.12.5761-5770.2001

Tecon, R., Or, D., 2017. Cooperation in carbon source degradation shapes spatial self-organization of microbial consortia on hydrated surfaces. Sci. Rep. 7, 43726. https://doi.org/10.1038/srep43726

Tropini, C., Earle, K.A., Huang, K.C., Sonnenburg, J.L., 2017. The gut microbiome: Connecting spatial organization to function. Cell Host Microbe 21, 433–442. https://doi.org/10.1016/j.chom.2017.03.010

Trovato, A., Seno, F., Zanardo, M., Alberghini, S., Tondello, A., Squartini, A., 2014. Quorum vs. diffusion sensing: a quantitative analysis of the relevance of absorbing or reflecting boundaries. FEMS Microbiol. Lett. 352, 198–203. https://doi.org/10.1111/1574-6968.12394

Varma, A., Palsson, B.O., 1994. Metabolic Flux Balancing: Basic Concepts, Scientific and Practical Use. Bio/Technology 12, 994–998. https://doi.org/10.1038/nbt1094-994

Xie, Z., Wroblewska, L., Prochazka, L., Weiss, R., Benenson, Y., 2011. Multi-input RNAi-based logic circuit for identification of specific cancer cells. Science 333, 1307–1311. https://doi.org/10.1126/science.1205527

Zomorrodi, A.R., Segrè, D., 2016. Synthetic ecology of microbes: mathematical models and applications. J. Mol. Biol. 428, 837–861. https://doi.org/10.1016/j.jmb.2015.10.019